

Pixelated VLC-backscattering for Self-charging Indoor IoT Devices

Sihua Shao, Abdallah Khreishah, Hany Elgala

Abstract—Visible light communication (VLC) backscatter has been proposed as a wireless access option for Internet of Things (IoT). However, the throughput of the state-of-the-art VLC backscatter is limited by simple single-carrier pulsed modulation scheme, such as on-off keying (OOK). In this paper, a novel pixelated VLC backscatter is proposed and implemented to overcome the channel capacity limitation. In particular, multiple smaller VLC backscatters are integrated to generate multi-level signals, which enables the usage of advanced modulation schemes. Based on experimental results, rate adaptation at different communication distances can be employed to enhance the achievable data rate. Compared to OOK, the data rate can be tripled when 8-PAM is used at 2 meters. In general, n -fold throughput enhancement is realized by utilizing n smaller VLC backscatters while incurring negligible additional energy using the same device space as that of a single large backscatter.

I. INTRODUCTION

It is expected that by 2020, the Internet will consist of 50 billion devices [1], which leads to imperative design of the Internet of Things (IoT). The IoT should be able to link every small object to the Internet and to enable an exchange of data never available before. However, several challenges need to be resolved for IoT. Connecting all these devices to the Internet through wire cables is impractical due to the deployment of wires, complexity added to the small IoT devices, and mobility of the devices. Thus the IoT devices are expected to be connected to Internet via wireless medium. Nevertheless, with the increase in the extremely large amount of wireless access devices, these IoT devices will compete with the users' devices on allocating the spectrum and the "spectrum crunch" [2] problem will be exacerbated if there is no innovative solution to significantly enhance the spectral efficiency. Furthermore, since it is impractical and cost-inefficient to replace the batteries of all these devices or power them through power cables, self-sustained operation enabled by energy harvesting needs to be utilized. The energy harvested from external sources is sufficient for the signal generation of IoT devices [3]. However, what can be harvested by IoT devices (in the order of 100 μ Watts) restricts the distance that transmitted signals can travel. Therefore, connecting to cellular networks or even WiFi is not usually a viable option. This distance constraint results in the requirement of huge infrastructure support, like access points and backhaul links, in order to achieve a small distance reuse factor. Also, trying to achieve such a small reuse factor causes the so-called "backhaul challenge" [4].

One proposed solution to the above challenges is to use RF-backscattering [5], [6]. Small IoT devices harvest energy

from the ambient RF signals broadcasted by TV towers [7] or WiFi signals generated by wireless routers, and modulate the reflected RF signals by varying the antenna's impedance, which affects the amount of signal that is reflected by the RF backscatter. While RF-backscattering provides an option for the Internet access of IoT devices, it has several inherent drawbacks. First, the uplink data rate depends on the amount of downlink traffic. For instance, in [5], in order to achieve an uplink data rate of 1 kbps, the WiFi router has to send at a data rate of more than 1.5 Mbps. In [6], it needs the downlink traffic at 24 Mbps in a range of 5 meters, to support the uplink data rate of 1 Mbps. Also, due to the omnidirectional propagation of the RF backscatter signals, interference among the RF backscatters and the uplink data traffic from the users' devices will be inevitable and destructive, especially when the number of IoT devices is large. Furthermore, since the maximum communication distance is short (e.g. 2-5 meters reported in [5], [6]), at least one access point needs to exist within this distance. This fact leads to the expensive infrastructure construction cost. One solution to this problem could be placing a reader [5], such as a mobile phone, within the maximum communication distance, which performs a signal relaying functionality between the access point and the IoT devices. However, this creates additional traffic from the reader, which competes with the mobile traffic and exacerbates the "spectrum crunch". Also, these readers might not exist all of the time and using mobile phones as readers might cause privacy problems. Another limitation of the RF-backscattering is that we might not be able to use it in a limited RF environment.

Due to the above-mentioned problems, another solution is introduced as the visible light communications (VLC) backscattering [8]–[11]. The VLC backscatter harvests energy from the existing indoor lighting infrastructure and performs modulation on the reflected light beam as long as the illumination is available. In Fig. 1, a small solar cell is used to harvest energy and a liquid crystal display (LCD) shutter, switching on or off, is used to modulated the reflected optical signals from a retro-reflector. This is motivated by the fact that whenever communication is needed illumination is also needed most of the time. Compared to RF backscatter, VLC backscatter solves the backhaul challenge by utilizing the existing infrastructure with slight modification [12]–[14] (i.e. adding driver and photodetector to the light source and utilizing the power line communication or power over Ethernet). Backscattering light beam is directional, which mitigates the interference problem. VLC backscatter does not require a reader to relay uplink data transmission. A shutter modulating the reflected light is proposed in [8] and the corner cube reflector maintaining the directionality of reflected beam is presented in [9], [10]. The state-of-the-art practical work that brings VLC backscatter into

Sihua Shao and Abdallah Khreishah are with the Department of Electrical and Computer Engineering, New Jersey Institute of Technology, email: ss2536@njit.edu, abdallah@njit.edu

Hany Elgala is with the Department of Computer Engineering, University at Albany, email: helgala@albany.edu

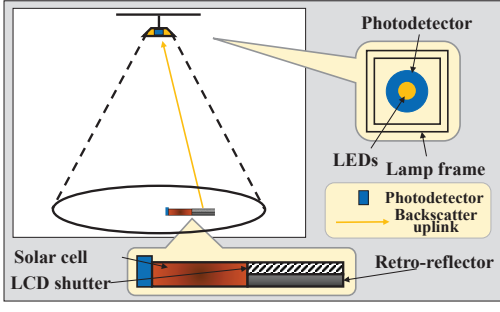


Fig. 1. VLC backscatter system architecture

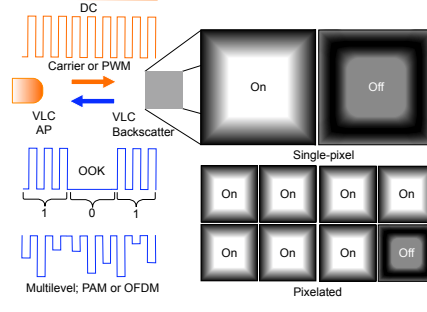


Fig. 2. The proposed pixelated based system

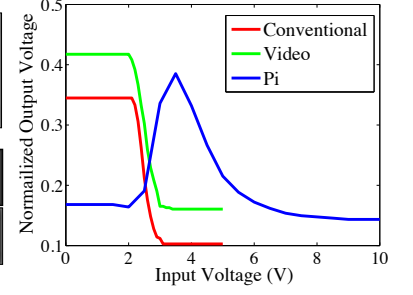


Fig. 3. IO curves for different LCD shutters

the IoT field is [11]. Nevertheless, no VLC backscatter system can leverage a modulation scheme that is more advanced than on-off keying (OOK). This is because the nonlinearity polarization of LCD shutters. The nonlinearity property of LCD shutters will be discussed in details in the next section.

In this work, we propose and implement a novel VLC backscatter, called pixelated VLC backscatter, which uses multiple smaller reflectors and LCD shutters to form numbers of pixels. Each pixel can switch on or off independently in order to produce multi-level signals. As shown in Fig. 2, with the same size of single pixel, pixelated backscatter utilizes more pixels by reducing the size of each pixel. Our proposed *pixelated* concept follows a similar concept as in [15] in terms of the contribution of multiple signals to form the effective communication signal. However, the motivation behind the LED based optical domain DAC in [15] is to be able to cover a wider dynamic range for a high peak-to-average-ratio (PAPR) orthogonal frequency division multiplexing (OFDM) signal, thus trading-off the elimination of the electrical digital-to-analog conversion (DAC) with higher complexity at the transmitter circuitry required to derive multiple LEDs. The main motivation of our independently designed work is allowing for the first time advanced modulation schemes in IoT using optical backscattering; multi-level (PAM) and multi-carrier (OFDM). Based on experiments, it is observed that the energy consumption of the pixelated design causes negligible overhead. Based on our testbed, the throughput achieved by the pixelated VLC backscatter is 600 bps at 2 meters, which is highly restricted by the response time of the off-the-shelf LCD shutters (5 ms). By reducing the size of LCD shutter, the capacitance of the LCD shutter is expected to decrease. According to [16], reducing the size of LCD shutters can potentially enhance the throughput by increasing the modulation frequency. Here, we do not customize the size of LCD shutters since we use the off-the-shelf samples.

II. NONLINEARITY POLARIZATION OF LCD SHUTTERS

Different from the impedance matching approach applied in RF backscatter [6], one LCD shutter is not capable of producing multiple (three or more) signal levels. To validate the nonlinearity property, we measure the transparency of three types of LCD shutters. Each type of LCD shutter is placed between a light source and a photodetector. By varying the drive voltage of the LCD shutters, we evaluate the transparency by measuring the output voltage of the photodetector. In Fig. 3, the output amplitude drops suddenly when the drive voltage reaches a certain level. Therefore, applying advanced

modulation schemes, such as pulse amplitude modulation (PAM) or OFDM, is not possible when single pixel VLC backscatter is used.

III. THEORETICAL ANALYSIS

In this section, we theoretically evaluate the benefit of adding pixels and the relationship between the maximum communication distance and the target BER. We also evaluate the amount of power that can be harvested for indoor environment.

A. BER vs. Communication distance vs. Number of pixels

In order to control the pixelated VLC backscatter while achieving a target backscattered signal quality, our main goal is to investigate the trade-off between the required number and size of pixels, signal-to-noise ratio (SNR) and resolution. Assume that the array, consists of identical pixels, i.e. when switched on, each pixel backscatters the same amount of

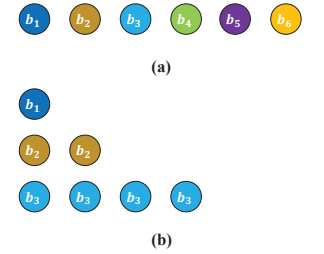


Fig. 4. Structure of pixels: (a) pixels with the same size; (b) binary-weighted clustering pixels

optical power proportional to incident optical flux on it, then the backscattered light is proportional to the number of pixels that are switched on (Fig. 4 (a)). In this case, 2^m optical levels can be achieved by switching 2^m pixels. To reduce the number of pixels with a given resolution, we can try to use a binary-weighted structure (Fig. 4 (b)) (Similar to the concept of Fig. 4 in [15]). In this case, the m^{th} cluster contains 2^{m-1} same-size pixels. In the following context, we refer to m instead of 2^{m-1} when we discuss the number of pixels, since the cluster of same-size pixels can be viewed as different-size pixels.

Here, PAM is considered as the modulation scheme. The 2^m optical levels enhance the bit rate by m times, when compared to the OOK, of which the bit rate is 1 bit/symbol. Given the symbol rate and assume the target BER is always satisfied, the throughput of m pixels based pixelated VLC backscatter is m times that of the single pixel. Since the IoT device is conceptually very small, assuming a certain area of VLC backscatter, we investigate the trade-off between the number of pixels and communication distance for a target BER.

Consider the M-PAM, the required number of pixels is $\log_2 M$. The relationship between BER and SNR is [17]

$$\text{BER} = \frac{2(M-1)}{M \log_2 M} Q\left(\frac{1}{M-1} \sqrt{\text{SNR}}\right) \quad (1)$$

where SNR denotes the square of the ratio of peak-to-peak amplitude and noise. Here we consider the noise as the worst case, which is the case that all the pixels are switched on. Since SNR is inversely proportional to the communication distance, it can be easily found that, given the BER, the number of pixels $\log_2 M$ is inversely proportional to the communication distance. Based on (1), we calculate the required SNR for different modulation schemes when the target BER is 10^{-3} and show the results in Table II.

B. Power harvesting

To evaluate the amount of power that can be harvested for indoor environment, we perform the following calculation: $P = E_{lux} \times I \times A \times E_{solar}$, where E_{lux} denotes the conversion ratio from lux to watt/cm², I denotes the illumination in unit lux, A represents the solar cell area, and E_{solar} represents the solar cell efficiency factor, we can find the electrical power P that can be generated by solar cell under indoor environment. We have $E_{lux} = 1.46 \times 10^{-7}$ watt/cm²/lux [18], $I = 300$ lux, and $A = 25$ cm². The solar cell efficiency 20% is generally available for commercialized solar cell products [19]. Substituting these values into the solar power calculation, the output $P = 219$ μ W.

IV. EXPERIMENTAL RESULTS

A. Testbed setup

The testbed consists of an 8.5 Watts white LED bulb, a microcontroller MSP430G2553 from Texas Instrument, 3 LCD shutters from Liquid Crystal Technologies, 3 super base ball stages, 3 cage mounted irises with diameter 20.0 mm and Photodetector PDA 36A from Thorlabs, 3 small mirrors, oscilloscope Tektronix MDO-4034, and a DC power supply.

The response time of the LCD shutters is around 5 ms, thus the maximum modulation frequency is set at 200 Hz. In [11], the response time of their LCD shutter is 2 ms, thus the effective bandwidth of their LCD shutter is larger than that of ours. The super base ball stages are used to control the azimuth and elevation angle of the pixels in order to perform the alignment. Since this testbed works as a proof-of-concept to investigate the performance of pixlated VLC backscatter, manually controlled positioners are used for orientation. The cage mounted irises are installed upon the LCD shutters to manipulate the area of each pixel. For instance, when one pixel is activated, the diameter is set at 20.0 mm; when two pixels are activated, the diameter of the 1st pixel is set at 16.33 mm, and the diameter of the 2nd pixel is set at 11.54 mm, to keep the total reflector area the same as that of one pixel. Note that by customizing the size of each pixel instead of controlling the reflector area through iris, the effective bandwidth of each pixel could be enhanced (i.e. above 200 Hz). Here, we use the off-the-shelf samples instead of customizing the size of the LCD shutters. The transmitted signals are pre-compiled in MSP430G2553 and this microcontroller is powered by a DC power supply with 3 V. The optical signals modulated by LCD shutters are captured by the photodetector and the waveform is displayed on the oscilloscope for further analysis. The VLC backscatter prototype, including the microcontroller MSP430 and three pixels, is shown in Fig. 5. For each pixel,

TABLE I
DCO/VLO OPERATE AT 3 V

Frequency	Current(DCO)	Current(VLO)
10 Hz	337 μ A	68 μ A
100 Hz	341 μ A	69 μ A
500 Hz	354 μ A	70 μ A

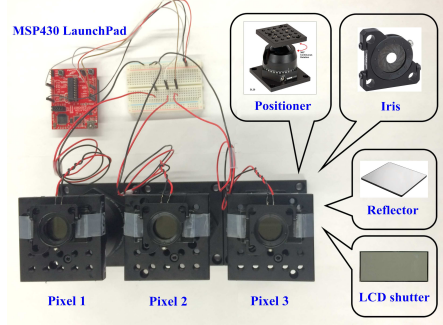


Fig. 5. Testbed of pixlated VLC backscatter

a LCD shutter is placed upon a reflector (i.e. mirrors), and a circular iris is fixed upon the LCD shutter to control the effective backscatter area.

B. Power consumption

First, we measure the power consumption of microcontroller and LCD shutter. The microcontroller consumes power in the order of magnitude 100 μ W while the LCD shutter consumes less than 0.2 μ W at 200 Hz (i.e. maximum modulation frequency). Therefore, the power consumption of the microcontroller is dominant in the VLC backscatter system.

The default clock module of MSP430G2553 is an internal digitally controlled oscillator (DCO) operating at 1 MHz. When the DC power supply provides 3 V, the current is around 340 μ A at 100 Hz (Table I). The required power ~ 1 mW is usually too high to be harvested from indoor illumination (~ 300 lux) by a small solar cell (e.g. 50 mm \times 50 mm). Since the maximum modulation frequency of the LCD shutter is only 200 Hz, the internal very-low-power low-frequency oscillator (VLO) is selected instead, of which the typical frequency is 12 kHz. With 3 V DC supply, the power consumption of the MSP430G2553 is reduced to around 200 μ W (Table I) when VLO is chosen. Compared to theoretical results in Section III B, the amount of power consumed by microcontroller (i.e. around 200 μ W) can be harvested from indoor lighting. Note that, in Table I, the impact of changing the frequency on power consumption is negligible.

C. Throughput vs. distance

We now start evaluating the trade-off between achievable throughput and the maximum communication distance, as discussed in the Section III. The number of pixels are varied from 1 to 3, corresponding to OOK, 4-PAM, and 8-PAM, respectively. The measurement distance is ranging from 2 meters to 5 meters. And the modulation frequency is set at 200 Hz, which means that the symbol rate is 200 symbols per second. The results for different number of pixels transmitting at 2 meters are shown in Fig. 6 to Fig. 8. Different signal levels are marked with the “ON” and “OFF” status of each

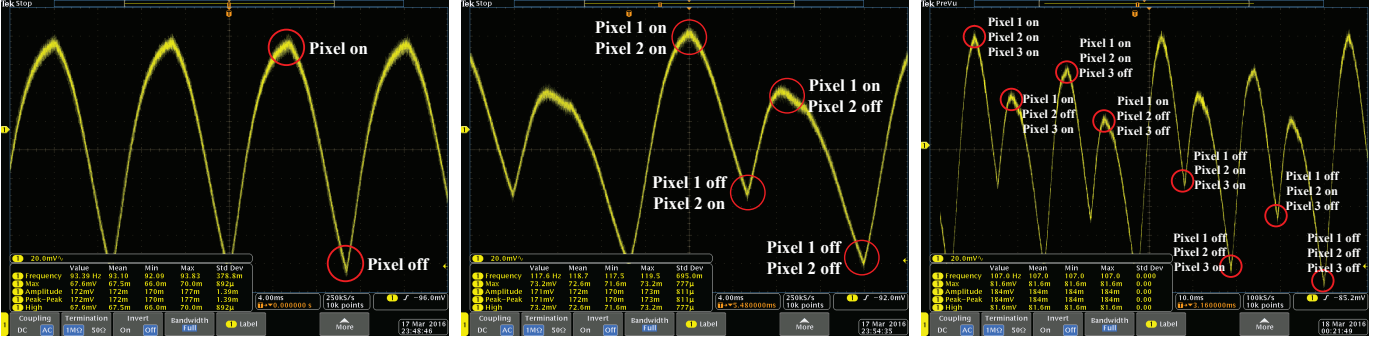


Fig. 6. Single pixel transmits at the distance of 2 meters and generates 2 signal levels Fig. 7. Two pixels transmit at the distance of 2 meters and generates 4 signal levels Fig. 8. Three pixels transmit at the distance of 2 meters and generates 8 signal levels

TABLE II
MODULATION SCHEME
VS. REQUIRED SNR

	OOK	4-PAM	8-PAM
Frequency	92.58 Hz	92.58 Hz	92.58 Hz
Amplitude	12.0mV	12.0mV	12.0mV
Peak-Peak	24.0mV	24.0mV	24.0mV
High	12.0mV	12.0mV	12.0mV
Low	0.0mV	0.0mV	0.0mV
Bandwidth	4.00m	4.00m	4.00m
Label	10k points	10k points	10k points

TABLE III
DISTANCE VS. SNR

Distance	2 m	3 m
OOK	26.55 dB	21.15 dB
4-PAM	18.80 dB	14.98 dB
8-PAM	18.80 dB	14.98 dB

pixel. Using unmodulated light beam on one end of the link to interrogate the pixelated VLC backscatter, the intensity of the backscattered signal depends on the number of pixels that are turned on or off. The backscattered intensities constructively add up, i.e. the backscattered signals are combined in the optical domain and not in the electrical domain. As it is observed from Fig. 8, the Euclidean distance of the constellation between different signal levels is still much larger than the noise when 8-PAM is applied. In Fig. 6, each signal level represents one bit and thus the achievable throughput is 200 bps. In Fig. 8, each signal level represents three bits and thus the throughput is increased to 600 bps. Therefore, with a relatively short communication distance, the M pixels based pixelated VLC backscatter is able to provide M times of the throughput of the single pixel VLC backscatter with negligible energy overhead and the same reflector area.

To evaluate the trade-off between achievable throughput and the maximum communication distance, we measure the SNR at different distances and show the results in Table III. Note that the SNR values measured at different distances are the same for OOK, 4-PAM, and 8-PAM. Compared to the results shown in Table II, we observe that the OOK modulation scheme can achieve the target BER above 5 meters, while the 8-PAM can only achieve the target BER at around 2 meters. Therefore, we can conclude that, based on our testbed, 600 bps can be achieved at 2 m, 400 bps can be achieved at 3 m, and 200 bps can be achieved at above 5 m. The higher order PAM is beneficial at shorter distance by doubling or even tripling the throughput, but has to sacrifice the maximum communication distance. This fact motivates performing the rate adaptation. Modulation scheme with small Euclidean distance of the constellation is used at short communication distance to enhance the achievable throughput, while modulation scheme with larger Euclidean distance of the constellation is used at longer distance to guarantee the robust connectivity.

V. CONCLUSION

In this work, a novel pixelated VLC backscatter system is implemented. With ultra-low power overhead, n pixels can

enhance the throughput by n times using the same reflector area when compared to single pixel VLC backscatter. Based on our experimental results and using 8-PAM, 600 bps is achieved at 2 meters and this data rate can be still greatly enhanced if customizing the size of each pixel is available. At short distance, high order PAM is preferred to provide high throughput while at longer distance, lower order PAM is needed to maintain the channel quality.

REFERENCES

- [1] Cisco, "Internet of Things (IoT)," <http://www.cisco.com/c/en/us/solutions/internet-of-things/overview.html>, [Online].
- [2] D. Hanchard, "FCC chairman forecasts wireless spectrum crunch," 2010.
- [3] S. Priya, *Energy harvesting technologies*. Springer, 2009.
- [4] S. Chia, M. Gasparroni, and P. Brick, "The next challenge for cellular networks: backhaul," *Microwave Magazine, IEEE*, 2009.
- [5] B. Kellogg, A. Parks, S. Gollakota, J. R. Smith, and D. Wetherall, "Wi-fi backscatter: Internet connectivity for rf-powered devices," in *SIGCOMM, ACM*, 2014.
- [6] D. Bharadia, K. R. Joshi, M. Kotaru, and S. Katti, "Backfi: High throughput wifi backscatter," in *SIGCOMM, ACM*, 2015.
- [7] V. Liu, A. Parks, V. Talla, S. Gollakota, D. Wetherall, and J. R. Smith, "Ambient backscatter: wireless communication out of thin air," *SIGCOMM, ACM*, 2013.
- [8] D. N. Mansell, P. S. Durkin, G. N. Whitfield, and D. W. Morley, "Modulated-retroreflector based optical identification system," Dec. 10 2002, uS Patent 6,493,123.
- [9] T. Komine, S. Haruyama, and M. Nakagawa, "Bidirectional visible-light communication using corner cube modulator," *IEIC Tech.*, 2003.
- [10] E. Rosenkrantz and S. Arnon, "Modulated retro reflector for VLC applications," in *SPIE Optical Engineering + Applications*. International Society for Optics and Photonics, 2014.
- [11] J. Li, A. Liu, G. Shen, L. Li, C. Sun, and F. Zhao, "Retro-VLC: Enabling battery-free duplex visible light communication for mobile and iot applications," in *HotMobile, ACM*, 2015.
- [12] S. Shao, A. Khreishah, M. B. Rahaim, H. Elgala, M. Ayyash, T. D. Little, and J. Wu, "An indoor hybrid WiFi-VLC internet access system," in *MASS, IEEE*, 2014.
- [13] S. Shao, A. Khreishah, M. Ayyash, M. B. Rahaim, H. Elgala, V. Jungnickel, D. Schulz, and T. D. Little, "Design and analysis of a visible-light-communication enhanced WiFi system," *JOCN, IEEE/OSA*, 2015.
- [14] M. Ayyash, H. Elgala, A. Khreishah, V. Jungnickel, T. Little, S. Shao, M. Rahaim, D. Schulz, J. Hilt, and R. Freund, "Coexistence of WiFi and LiFi towards 5G: Concepts, opportunities, and challenges," *IEEE Communication Magazine*, 2016.
- [15] J. Armstrong, "Optical domain digital-to-analog converter for visible light communications using led arrays [invited]," *Photonics Research*, vol. 1, no. 2, pp. 92–95, 2013.
- [16] K. Y. Ahn, "Method of fabricating integrated circuit wiring with low RC time delay," Mar. 14 2000, uS Patent 6,037,248.
- [17] S. Hranilovic, *Wireless optical communication systems*. Springer Science & Business Media, 2006.
- [18] "Lux to Watt/square centimeter Conversion," http://www.endmemo.com/sconvert/luxwatt_squarecentimeter.php, [Online].
- [19] Shawn, "Top 20 Most Efficient Solar Panels," <http://sroeco.com/solar/top-20-efficient-solar-panels-on-the-market/>, [Online].